Sensors & Actuators: A. Physical 374 (2024) 115519

Contents lists available at ScienceDirect

Sensors and Actuators: A. Physical

journal homepage: www.journals.elsevier.com/sensors-and-actuators-a-physical

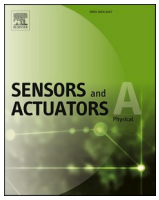

Capacitive PVC gel pressure sensors with various interlinked microstructural dielectric middle layers

Chen Liu, Muhammad Hassan Uddin, Ketao Zhang *

School of Engineering and Materials Science, Queen Mary University of London, Mile End, London, England E1 4NS, UK

ARTICLE INFO

Keywords:
Microstructure
Bending
PVC
Capacitive sensor

ABSTRACT

Our sharp tactile sense is largely attributable to an undulating layer of microstructures between the epidermis and dermis, amplifying tactile signals. Taking inspiration from the biological template, we propose a design of flexible capacitive pressure sensors with various microstructural dielectric middle layers, fabricated using a casting-based approach. This is the first confirmed use of microstructural polyvinyl chloride (PVC) gel in dielectric layers and the first example of casting in the fabrication of capacitive sensors. Notably, on account of its flexibility, the sensor also addresses the problem of microstructure fracture and misalignment during sensor bending. These sensors can achieve a maximum sensitivity of 1.34 kPa^{-1} (under 10 kPa) with a fast response time (50 ms), good cyclic stability (> 1000 cycles), and a wide pressure sensing range (0 ~ 290 kPa). When attached to a cup or balloon, this study reveals that these sensors can detect the weight and rigidity of the objects, demonstrating their potential in human-machine interaction, as well as in wearable applications.

1. Introduction

Electronic skin (E-skin), which mimics the sensory functions of human skin, is a new type of flexible wearable sensor with skin-like characteristics of thinness, softness, and flexibility [1–3]. It can transform external stimuli into a variety of output signals (such as capacitance, resistance, or light intensity) and therefore has broad application prospects in the fields of intelligent medical care [4,5], human-machine interaction (HMI) [6,7], virtual reality (VR) [8,9], and artificial intelligence (AI) [10,11]. Electronic skin needs the basic capabilities of sensation and touch in order to sense different external pressures and relay tactile signals as is the case in human skin [12–14].

As the core building blocks of E-skins, pressure sensors can be categorized into certain types on the basis of their sensing mechanisms [15,16]: which can be piezoresistive [17,18], capacitive [19–22], piezo-electric [23,24], optical [25,26], triboelectric [27–29], and magnetic [30,31]. Due to their low power consumption, simple structure, promising dynamic characteristics, and resistance to disturbance, capacitive sensors have attracted much attention. Flexible capacitive sensors typically have a “sandwich” structure, consisting of two electrode layers with a dielectric layer in the middle. Research has found this to be key to improving the sensitivity of the sensor, with many researchers now looking at how its design could optimize performance [32–34].

A key factor in skin’s high sensitivity to touch is the presence of microstructures between the epidermis and dermis, which, as shown in Fig. 1(a), have a corrugated profile and amplify external pressure [35]. To mimic that property of the skin, researchers have designed capacitive sensors with microstructures, greatly improving sensitivity [36,37]. Currently, there are two main types of the fabrication process: (1) using photolithography to fabricate microstructure templates equipped with pyramids [38] or columns [39], and then transferring them to a flexible polymer dielectric layer; (2) using natural biomaterials (e.g. banana leaves [40], lotus leaves [41]) as templates to fabricate microstructure arrays. The prior approach has high preparation accuracy and good microstructure controllability while it is complex and expensive. The latter method is simple and highly efficient, but the morphology of the microstructures is almost completely non-adjustable, and the optimization is therefore limited [42]. Because these sensors operate under extreme conditions (i.e. bending), and the dielectric and electrode layers are not manufactured as a single unit, slippage can cause misalignment, affecting sensor performance [43,44]. There is an urgent need to identify a simple, efficient, and stable microstructure preparation process. In this work, we develop a type of polyvinyl chloride (PVC) gel-based capacitive sensors with various microstructural dielectric middle layers, as shown in Fig. 1(b) and (c), the electrodes are 0.3 mm thick

* Corresponding author.
E-mail address: ketao.zhang@qmul.ac.uk (K. Zhang).

https://doi.org/10.1016/j.sna.2024.115519
Received 16 January 2024; Received in revised form 4 May 2024; Accepted 21 May 2024
Available online 22 May 2024

stainless steel sheets (304 stainless steel, Sourcing Map Company, UK) for good conductivity and integration with PVC gel material. Prior to this work, PVC gel had mainly been used in actuator designs [45–47], and very few studies have been done on its capacitive sensing properties [48,49]. PVC gel has a small modulus of elasticity, a large dielectric constant, and properties that are insensitive to humidity and temperature [50], making it ideal for use in the dielectric middle layer of a capacitive pressure sensor [51].

2. Design and fabrication

A conventional sensor design based on microstructure is shown in Fig. 2(a). There is an air gap between the electrode layer and the dielectric layer. When subjected to bending, the dielectric and electrode layers of the sensor separate further, resulting in the possibility of misalignment leading to poorer performance [43], as shown in Fig. 2(b). In our novel design, a dielectric material (PVC gel) is wrapped around the entire sensor, fully binding the dielectric and electrode layers, as shown in Fig. 2(c) and (d). When the sensor undergoes deformation through bending, the layers are held tightly together, regardless of whether the dielectric layer is a triangular microstructure (Fig. 2(e)) or an hourglass-shaped microstructure (Fig. 2(f)).

In this work, we also developed a simple and reliable manufacturing process, as shown in Fig. 2(g). The process starts with casting the PVC gel solution to cover the two electrodes and a mask, which is 3D printed using a printer (Formlabs 3+, US) with a high accuracy of 0.01 mm. The mask is then removed to form the microstructural dielectric layer. To solve the problem of its adhesion to the PVC gel when removing the mask plate, we immerse the printed plate into 40 % polyvinyl alcohol (PVA) solution and remove it after 10 s, then apply a surface coating of PVA film, which is a few micrometers thick. This water-soluble film perfectly separates the mask plate from the cured PVC gel.

3. Results and discussion

3.1. Simulation of the pressure

One of the key objectives of this work is to improve the sensor's sensitivity (S), which is usually defined as the tangent slope of the curve (change in capacitance relative to the applied pressure) and can be expressed as [52]

$$S = \frac{\Delta C/C_0}{P} \tag{1}$$

where ΔC is the change of the capacitance, C_0 is the initial capacitance, and P is the vertical pressure applied to the sensor. The pressure is a function of the elastic modulus of the dielectric layer (compression modulus)

(E) and the change of the distance(Δd), expressed as [53]

$$P = E{\cdot}\Delta d = E{\cdot}(d - d_0) \tag{2}$$

where d is the distance between the two electrodes under applied pressure and d_0 is the initial distance (1.4 mm).

Therefore, when $\Delta C/C_0$ is a constant, the sensor is more sensitive with a smaller P (the smaller E). Assuming other parameters are the same, this suggests that the sensor with the dielectric middle layer of lower elastic modulus has higher sensitivity than the one with higher elastic modulus.

To achieve a dielectric middle layer with a low elastic modulus, we use finite element analysis (FEA) in Abaqus to compute the stress on three structures of dielectric units, as shown in Fig. 3(a), setting the modulus of the PVC gel material to 200 kPa [51,54]. Three structures of PVC gel are compressed to the same displacement (1 mm). The result indicates that the solid structure exhibited the most notable slope (K = 0.042), followed by the triangular structure (K = 0.013). The hourglass-shaped structure showed a slightly lower slope (K = 0.012), with minimal distinction between the latter two. This implies that dielectric units with a microstructure design are more susceptible to compression and are likely to be more sensitive.

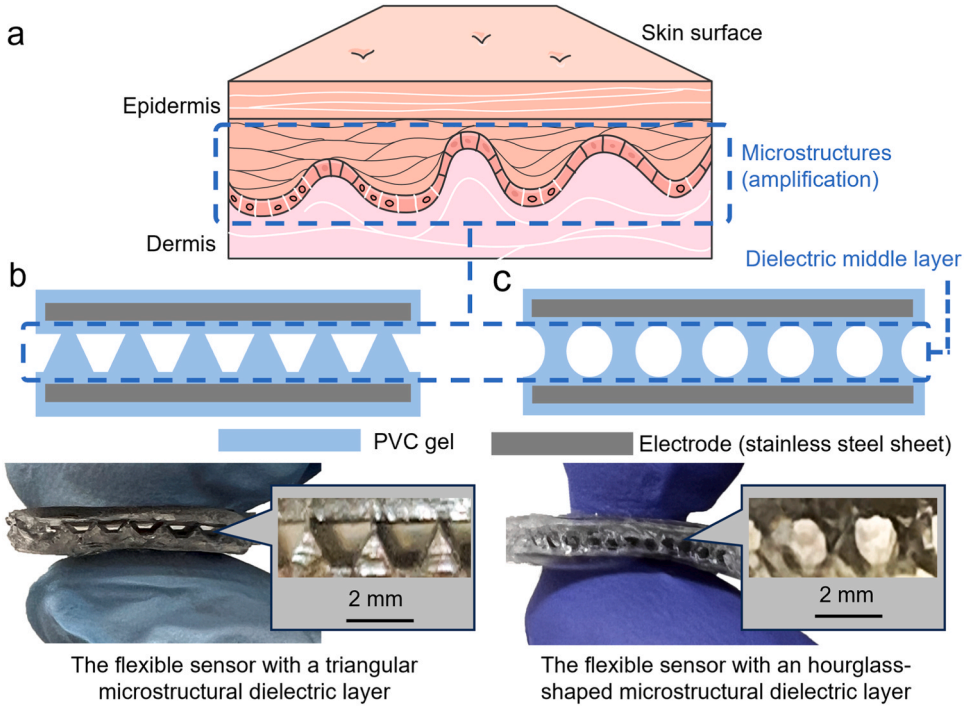

Fig. 1. Capacitive sensors inspired by human skin. (a) Schematic representation of the structural components of the skin: epidermis, microstructure, and dermis. (b) The PVC gel capacitive sensor with a triangular skeletonized dielectric layer. (c) The PVC gel capacitive sensor with an hourglass-shaped skeletonized dielectric layer.

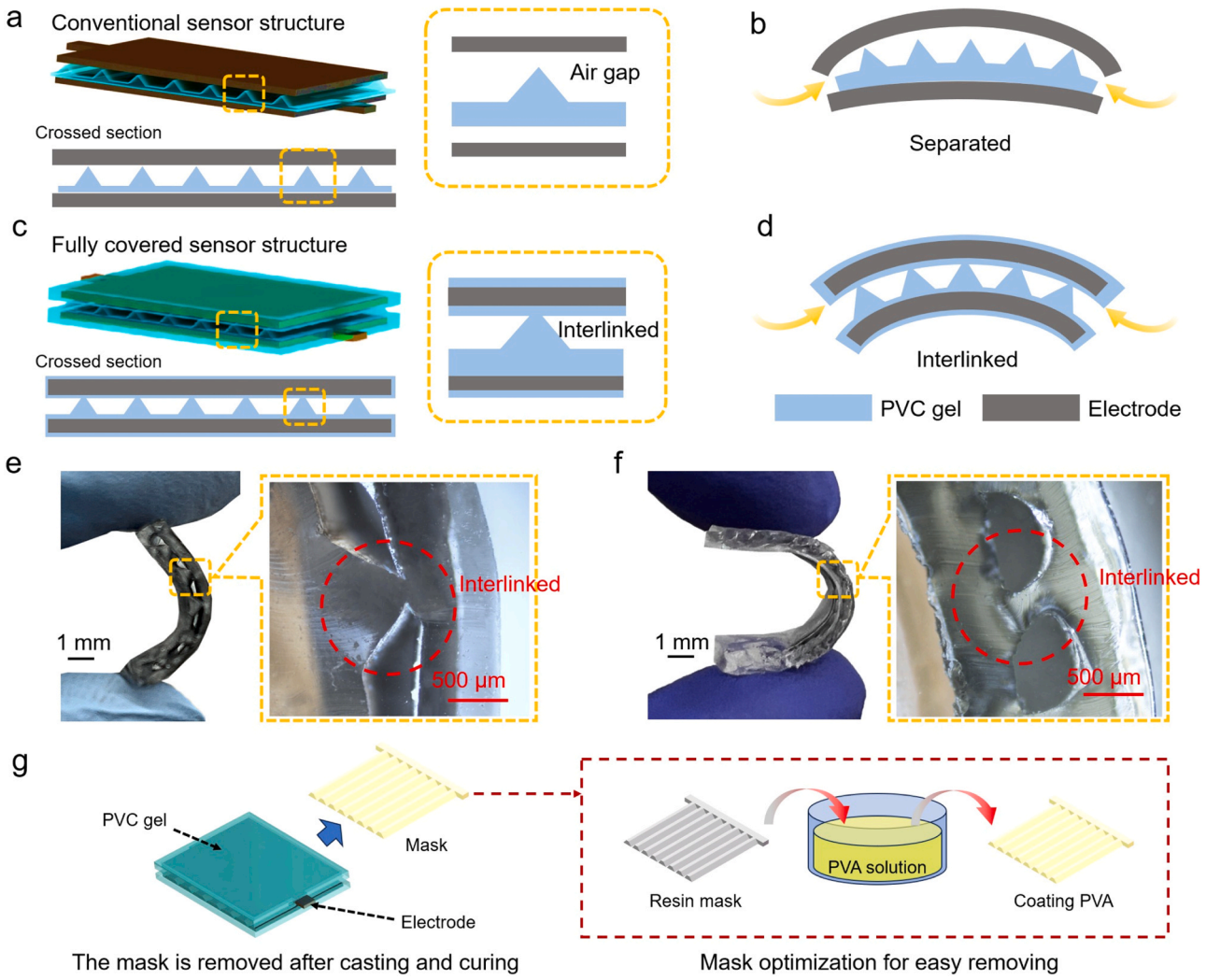

Fig. 2. Interlinked dielectric layers guarantee the stability of the sensor. (a) The dielectric layer structure of conventional sensors has air gaps between layers. (b) When a conventional sensor is bent, the dielectric layer easily separates from the electrodes. (c) The fully covered sensor structure in this work bonds the layers. (d) The fully covered bonded sensor keeps layers stable when bent. (e) The cross-section of the sensor with the triangular microstructural dielectric layer when it is bending. (f) The cross-section of the sensor with the hourglass-shaped microstructural dielectric layer when bending. (g) The sensor is made by casting PVC gel solution to cover two electrodes, and a mask is applied to form the microstructural dielectric layer. The mask covered with PVA can be easily removed from the cured PVC gel.

In light of this, we designed sensors with triangular and hourglass-shaped dielectric layers to compare their elastic modulus, as shown in Fig. 3(b). We also categorized the dielectric layer design into three types based on the PVC gel volume fractions (V_P) of 20 %, 35 %, and 50 %, as also shown in Fig. 3(b). Fig. 3(c) displays the results for the 35 % version (refer to the simulation video in the Supporting Information). The results shown in Fig. 3(d) reveal that for the same distance of compression (1 mm), the compressive stress also decreases when the V_P decreases. We also note that the dielectric layer with the hourglass-shaped microstructure is easier to compress than the layer with the triangular microstructure at the same V_P.

However, E is not the only factor affecting sensitivity. The dielectric constant of the dielectric layer is another key factor that significantly influences the capacitance change.

3.2. Components analysis of the PVC gel

For a capacitive sensor, its capacitance (C) is given by [55]

$$C = \varepsilon \frac{A}{4k\pi d} \tag{3}$$

where C is the capacitance, ϵ is the dielectric constant of the dielectric layer, A is the effective area of the two electrodes, and k is the electrostatic force constant.

The PVC gel volume fraction (V_P) not only affects the elastic modulus (E) but also the dielectric constant ε, as defined by [34]

$$\varepsilon = V_{air}\varepsilon_{air} + V_P\varepsilon_P \tag{4}$$

where V_{air} and V_P are the volume fractions ($V_{air} + V_P = 1$) of air and PVC gel, respectively. ε_{air} and ε_P are the dielectric constants of the air and PVC gel, respectively, and $\varepsilon_P > \varepsilon_{air}$.

The ε_P is adjusted by the components ratio of the PVC gel. The PVC gel comprises PVC and dibutyl adipate (DBA). Through our experiments, we established that different composition ratios of these two materials led to different elastic moduli and dielectric constants, as shown in Fig. 4. The result demonstrates that increasing the weight ratio of DBA (mDBA) in the gel leads to a decrease in the modulus of elasticity and an increase in the dielectric constant. This suggests that employing a higher weight ratio of DBA to fabricate the PVC gel dielectric layer can enhance the sensitivity of the capacitive pressure sensor. However, in the fabrication process, when mPVC:mDBA is 1:8 and 1:10, it is difficult to

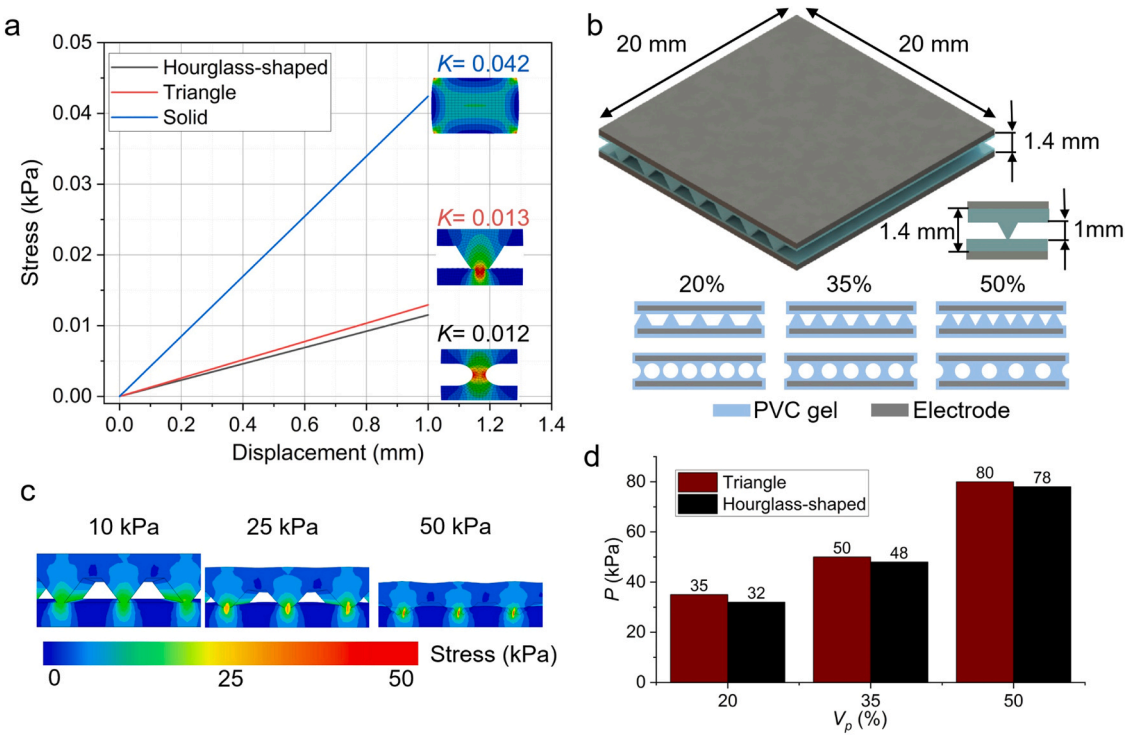

Fig. 3. Force simulations of the various structural sensors. (a) The stress simulation of a single unit for three structures (hourglass- shaped, triangular, and solid). (b) The dimensions of one sensor unit and schematics of various cross sections of different gel ratios and structures. (c) The simulation effect of the sensor with a triangular 35 % gel structure. (d) Simulation results for two dielectric layer structures (triangular and hourglass-shaped) in three various gel ratios (20 %, 35 %, and 50 %).

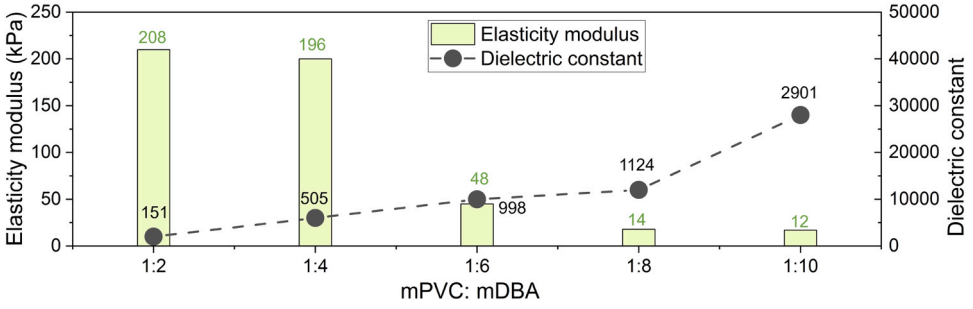

Fig. 4. Elastic modulus and dielectric constant of dielectric layers with various mass ratios of PVC and DBA.

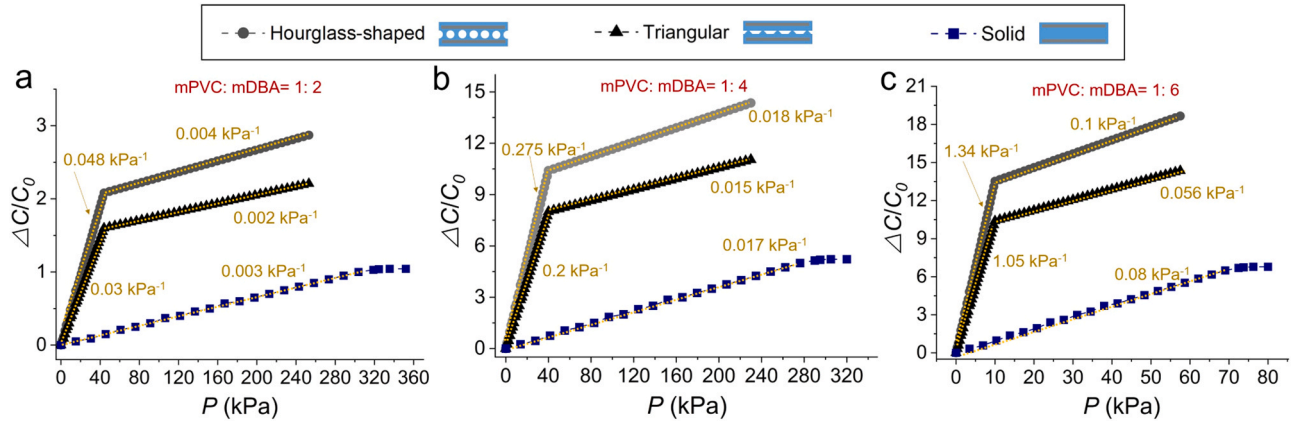

Fig. 5. Testing results. (a) Sensor sensitivity test results of three dielectric layer structures (hourglass-shaped, triangular, solid) with three different composition ratios: mPVC: mDBA = 1: 2; (b) mPVC: mDBA = 1: 4; (c) mPVC: mDBA = 1: 6.

maintain the microstructural morphology in the dielectric layer because the elastic modulus is too low. Furthermore, it is difficult to recover previous morphology having been pressed with even a small amount of pressure (2 kPa) due to high viscosity. Therefore, those two proportions of dielectric layer constituents are clearly unsuitable.

3.3. Tests of sensors

To investigate the combined effects of V_P, material composition ratio, and microstructure geometry design on the sensor's performance, we prepare three structures (solid, triangular, and hourglass-shaped) with V_P of 20 %, 35 %, and 50 % and mPVC:mDBA of 1:2, 1:4, and 1:6, respectively, and test them separately. The pressure test equipment (Instron 3342, Instron, UK) is used to apply downward pressure and displacement to the sensors while recording these data. The change in capacitance of the sensor ($\Delta C/C_0$) is collected by the computer through the LCR meter (LCR-6002, RS components, UK). (Please see the schematic of the testing platform in the supporting information.)

The relationship between pressure (P) and ($\Delta C/C_0$) is shown in Fig. 5 (b), (c), and (d), which present test results for the condition of 35 % PVC gel fraction in the dielectric layer. These three plots represent the results of the sensor sensitivity tests at mPVC:mDBA of 1:2, 1:4, and 1:6, respectively. The results show that the sensor with more DBA in the dielectric middle layer has a more extensive pressure range. This is because the PVC gel with more DBA has a larger modulus. The results also demonstrate that both the hourglass-shaped and triangular microstructured sensors have two phases of sensitivity, in each case the sensitivity at the beginning of the compression being much higher than that of the sensor with a solid dielectric layer. Fig. 5(b), (c), and (d) also show that in the compression process, the sensitivity is high at the stage when the microstructure is initially compressed (δd: 0 ~ 1 mm), and the compressive stress is low. When the microstructure layer is completely compressed ($\delta d > 1$ mm), the dielectric layer acts as a solid structure, and as the compressive stress increases, sensitivity decreases. The results also show that as the mDBA increases, sensitivity also increases. The sensor with the hourglass-shaped microstructural dielectric layer has greater sensitivity than the triangular one, further validating the simulation results (the sensor with the hourglass-shaped microstructural dielectric layer has a smaller modulus), shown in Fig. 3.

Having measured all the sensor readings for each component ratio, PVC gel fraction, and for each dielectric layer microstructure, the data was compiled as shown in Table 1. The maximum compression displacement for each sensor was the same, set at 1 mm in each case. As the proportion of PVC gel increases from 20 % to 50 %, the measurable ranges for all sensors with microstructural dielectric layers also increase. We see from the data that the most sensitive sensor (1.34 kPa^{-1}) is the one with a 35 % hourglass-shaped microstructural layer and a mPVC: mDBA ratio of 1:6. The corresponding stress measurement range is 0 ~ 10 kPa. The broadest measurable range exhibited was 0 300 kPa in the case of a solid PVC gel dielectric layer with an mPVC: mDBA ratio of 1:2.

To evaluate the sensor's stability in performance under bending conditions, we selected the sensor with a maximum sensitivity of 1.34 kPa^{-1} for bending and compression-release cycle tests. When the sensor is compressed on the Instron 3342 to various bending angles from 0° to 120°, as shown in Fig. 6(a), the results show that the sensor can perform consistently when it is bending to a specific angle. In addition, we find that as the bending angle increases, sensitivity decreases. This is due to the microstructural dielectric layer thickening when stretched, and, as there is a pre-stretching force during bending, the compressive stress also increases. The sensor maintains stable sensitivity even at bending angles up to 120° (the bending radius β is 4.1 mm), but when the bending angle is up to 150° (the bending radius β is 1.6 mm), it causes excessive stretching and leads to breaks in the dielectric layer, which makes the sensitivity unpredictable. In addition, we also conducted the cycle test (up to 2000 times) of compressing and releasing the sensor at 1 Hz, as shown in Fig. 6(b). It illustrates the sensor's stable repeatability with a maximum error of 2.95 kPa.

Table 1
The sensitivities among various dielectric gel structures and components ratios.

V_P	mPVC: mDBA	S (Solid)/kPa^{-1}	S (Triangle)/ kPa^{-1}	S (Hourglass-shaped)/kPa^{-1}
20 %	1: 2	0.003 (0 ~ 300 kPa) (100 % gel)	0.025 (0 ~ 35 kPa)	0.03 (0 ~ 33 kPa)
			0.001 (35 ~ 190 kPa)	0.003 (33 ~ 190 kPa)
	1: 4	0.017 (0 ~ 275 kPa) (100 % gel)	0.15 (0 ~ 30 kPa)	0.2 (0 ~ 29 kPa)
			0.01 (30 ~ 200 kPa)	0.015 (29 ~ 200 kPa)
	1: 6	0.08 (0 ~ 73 kPa) (100 % gel)	0.6 (0 ~ 6 kPa)	0.8 (0 ~ 5 kPa)
			0.04 (6 ~ 55 kPa)	0.1 (9 ~ 55 kPa)
35 %	1: 2	0.003 (0 ~ 300 kPa) (100 % gel)	0.03 (0 ~ 40 kPa)	0.048 (0 ~ 38 kPa)
			0.002 (40 ~ 260 kPa)	0.004 (38 ~ 260 kPa)
	1: 4	0.017 (0 ~ 275 kPa) (100 % gel)	0.2 (0 ~ 35 kPa)	0.275 (0 ~ 33 kPa)
			0.015 (35 ~ 220 kPa)	0.018 (33 ~ 220 kPa)
	1: 6	0.08 (0 ~ 73 kPa) (100 % gel)	1.05 (0 ~ 10 kPa)	1.34 (0 ~ 10 kPa)
			0.056 (9 ~ 58 kPa)	0.1 (9 ~ 58 kPa)
50 %	1: 2	0.003 (0 ~ 300 kPa) (100 % gel)	0.025 (0 ~ 70 kPa)	0.042 (0 ~ 68 kPa)
			0.003 (70 ~ 290 kPa)	0.003 (68 ~ 290 kPa)
	1: 4	0.017 (0 ~ 275 kPa) (100 % gel)	0.14 (0 ~ 65 kPa)	0.25 (0 ~ 64 kPa)
			0.011 (65 ~ 250 kPa)	0.012 (35 ~ 250 kPa)
	1: 6	0.08 (0 ~ 73 kPa) (100 % gel)	0.5 (0 ~ 20 kPa)	0.7 (0 ~ 17 kPa)
			0.06 (9 ~ 58 kPa)	0.08 (9 ~ 58 kPa)

3.4. Two demonstrations

We carried out experimental tests to demonstrate two applications of the sensor in our daily lives – specifically relating to sensing the weight in different temperatures and rigidity of an object.

1) To illustrate the sensor's capability in detecting weight changes of grasped items across different temperatures, we integrated the proposed sensor, with a maximum sensitivity of 1.34 kPa^{-1}, into a rubber finger cot, as shown in Fig. 7(a). The participant who wore the cot picked up the non-transparent cup, held it for 10 s, and then placed it back, repeating this cycle 3 times, each time with a different amount of water in the cup. In Fig. 7(a), it can be observed that the variation in $\Delta C/C_0$ of the capacitive sensor across three different test scenarios: when the cup is 30 % filled, the $\Delta C/C_0$ is 1.5; when the cup is 60 % filled, the $\Delta C/C_0$ is 3.3; when the cup is 90 % filled, the $\Delta C/C_0$ is 4.8. The greatest change in capacitance occurred when the participant held the heaviest object. This suggests that our flexible sensor effectively detects fingertip pressure levels during grasping actions. The capacitive signal was recorded using the LCR meter at 10 kHz frequency to obtain response (50 ms) and recovery (120 ms) time. After that, the participant repeated this demonstration with 60 % water of various temperatures in the cup to check the sensor's performance, as shown in Fig. 7(b). The temperature of the cup wall was measured by using an infrared thermometer (Gm550, Benetech, China). The results show that the sensor can keep a stable performance in a range of various temperatures between 4 (iced water) and 90 °C (hot water).

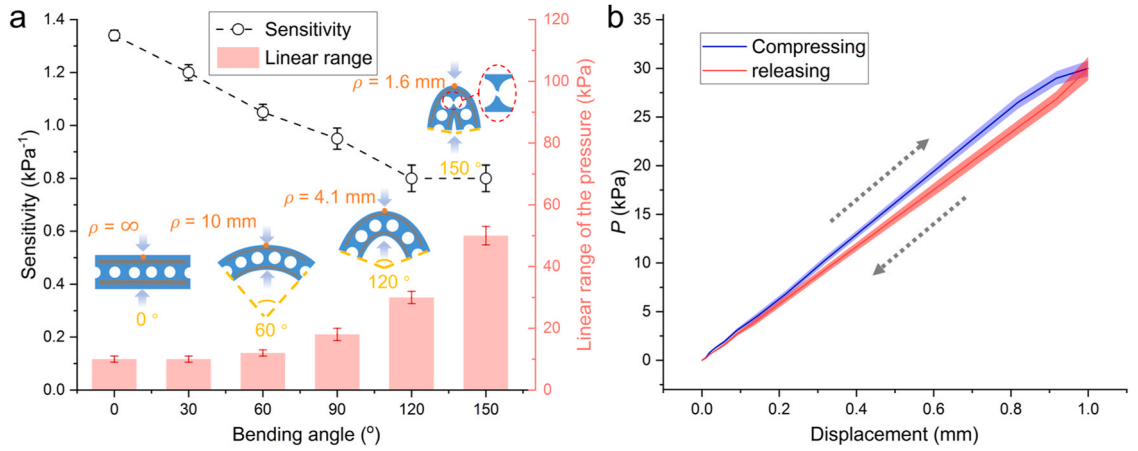

Fig. 6. (a) The sensitivities of the sensor when it is bent between 0° and 150°. (b) The sensor's mechanical properties remain stable even after undergoing 2000 compression-release cycles.

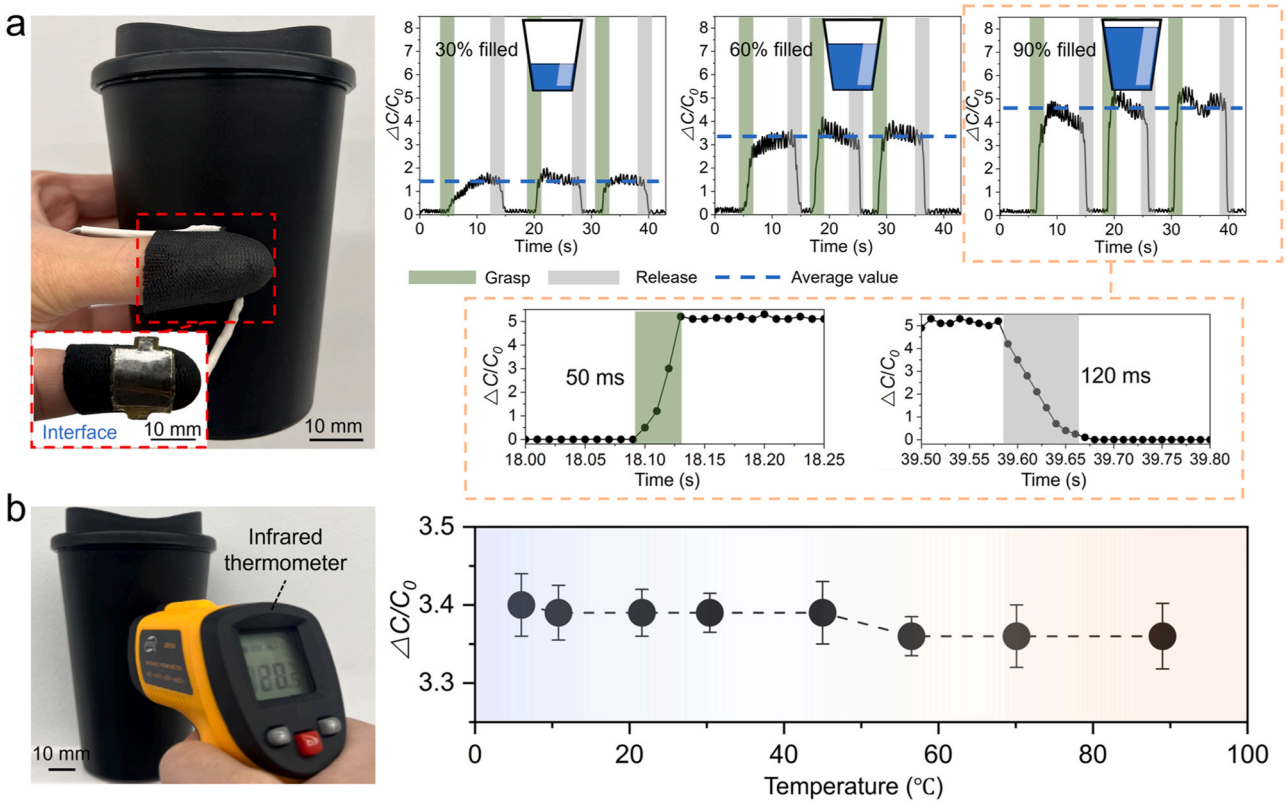

Fig. 7. Demonstrations of the sensor attached to a cup: (a) When the participant holds the cup filled with water to three different volumes, the sensor attached to the side of the cup can detect the corresponding weight, respectively. (b) When the participant holds the cup filled with 60 % water at various temperatures, the sensor can keep a stable performance.

2) To showcase the sensor's ability to detect changes in surface stiffness, we affixed it to an uninflated rubber balloon (10-inch, SQQ0100-JJ XLUK, Jc.upin). The sensor is used to detect the contact pressure applied and to derive from that, the air pressure inside the balloon, as shown in Fig. 7(b). In this demonstration, an Instron 3342 was used to press the sensor attached to the balloon. We set the compression speed to 5 mm·min^{-1} and the displacement to 1 mm. The balloons were inflated to three volumes 8000 cm^3, 3400 cm^3, and 1000 cm^3, respectively, and were placed on the Instron 3342 for testing. The sensor calculates $\Delta C/C_0$ as 1.5, 2.5, and 4.7, respectively, as shown in Fig. 8. The results show that the higher the air pressure inside the balloon, the greater the stiffness and, in turn, the greater the contact pressure. It also demonstrates the sensor's high sensitivity that enables it to detect a small compressive stress of 1.6 kPa, which is even smaller than human skin modulus (10 kPa ~ 200 MPa) [56,57].

3.5. Comparison with other flexible capacitive pressure sensors

Comparing the performance with other recent flexible capacitive sensors, as shown in Table 2, the proposed capacitive sensor with microstructural PVC gel dielectric layers balances response, sensitivity, measurement range, and bending resistance. In particular, it offers the highest resistance to bending (it can withstand bending angles of up to

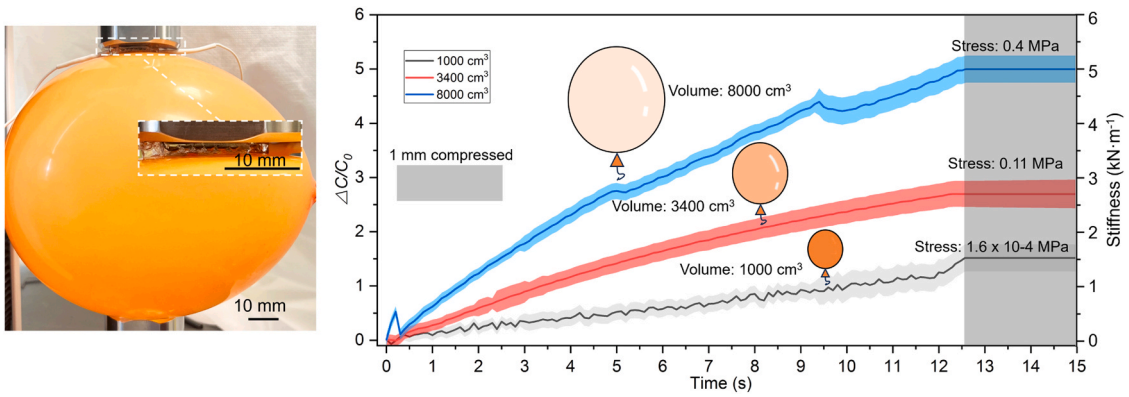

Fig. 8. Demonstrations of the sensor attached to a balloon: the sensor can detect different hardness levels of an inflated balloon when the balloon is squeezed by an external load applied to the sensor attached to the balloon.

Table 2
Comparison with other flexible capacitive pressure sensors.

Name of sensors	Dielectric layer	Response time	Max sensitivity/kPa^{-1}	Range/kPa	Bending/°
Pyramidal capacitive sensor [38]	PDMS	1.3 s	1 (0~50 kPa)	0~1100	N/A
3D printed sensor [33]	AgNW-TPU	100 ms	1.21 (0~2.8 kPa)	0~28	N/A
PDMS-CNTs pressure sensor [43]	PDMS-CNT	6 ms	0.15 (0~47 kPa)	0~450	45
Micropatterned sensor [42]	Polyimides	36 ms	1.2 (0~2 kPa)	0~20	90
Flexible capacitive sensor [58]	PVA-KHO	50 ms	20.83 (0~5 kPa)	0~5	N/A
Phlebothrombosis monitor [59]	PDMS-MWCNT	90 ms	2.16 (50 Pa~2 kPa)	0~500	N/A
All-fabric capacitive sensor [60]	CNT-PDMS	27.3 ms	8.31 (0 Pa~1 kPa)	0~80	60
MXene/PVP based sensor [61]	MXene-PVP	15 ms	1.25 (130 Pa~98 kPa)	0~294	90
This work	PVC gel	50 ms	1.34 (0~10 kPa)	0~290	120

*PDMS: polydimethylsiloxane; AgNW: silver nanowire; TPU: thermoplastic polyurethane; CNT: carbon nanotube; PVA: polyvinyl alcohol; KHO: potassium hydroxide; MWCNT: multi-walled carbon nanotubes; MXene: 2D transition metal carbide and nitride; PVP: polyvinylpyrrolidone.

120°) compared to other works.

4. Conclusion

Inspired by the interlinked microstructures between the dermis and epidermis in human skin, this work developed a simple method, combining 3D printing and PVC gel casting techniques, to fabricate sensitive and flexible capacitive pressure sensors with morphology-controllable dielectric middle layers. This is the first time PVC gel has been used for the microstructural dielectric intermediate layer in capacitive sensors. The FEA simulations and experimental results of sensor prototypes show that due to the high dielectric properties and microstructural design of PVC gel, the highest sensitivities can reach 1.34 kPa^{-1} within a monitoring range of 0 ~ 10 kPa. The results also proved that the proposed fabrication method of using 3D-printed moulds soaked in PVA solution ensures the smooth removal of the mask and moulding stability of the microstructures. Furthermore, the integrated casting approach enables a strong bond between the microstructural dielectric middle layer and electrode layers. This prevents structural misalignment when the sensor is subjected to bending and deformation (the allowed maximum bending angle is up to 120°, and the bending radius is 4.1 mm), thus guaranteeing operational stability. The proposed fabrication process ensures the consistent performance of these sensors under different bending configurations. Ultimately, we demonstrated the sensor's potential as a wearable interface by affixing it to a rubber finger cot to detect changes in the cup's weight. Additionally, it can also be used to detect the rigidity of an object in contact with the sensor.

Author Statement

The authors declare that:

the work described has not been published previously;
it is not under consideration for publication elsewhere;
its submission is approved by all authors;
during the preparation of this work, the author did NOT use generative artificial intelligence (AI) and AI-assisted technologies.

CRediT authorship contribution statement

Chen Liu: Writing – original draft, Software, Resources, Methodology, Investigation, Formal analysis, Data curation, Conceptualization. **Ketao Zhang:** Writing – review & editing, Supervision, Project administration. **Muhammad Hassan Uddin:** Software, Data curation.

Declaration of Competing Interest

The authors declare that they have no known competing financial interests or personal relationships that could have appeared to influence the work reported in this paper.

Data availability

Data will be made available on request.

Acknowledgements

This work is supported in part by the Royal Society International Exchanges Cost Share award under grant agreement (IEC\NSFC \211324), Innovate UK award under grant agreement (10074371), and Queen Mary University of London - China Scholarship Council (QMUL-CSC) Scholarship. The authors would like to thank Mr. Mish Toszeghi for proofreading the manuscript and thank Dr. Abu Bakar Dawood, and Mr. Eisa Anwar for providing testing devices.

Appendix A. Supporting information

Supplementary data associated with this article can be found in the online version at doi:10.1016/j.sna.2024.115519.

References

[1] F. Liu, S. Deswal, A. Christou, M. Shojaei Baghini, R. Chirila, D. Shakthivel, M. Chakraborty, R. Dahiya, Printed synaptic transistor–based electronic skin for robots to feel and learn, Sci. Robot. 7 (67) (2022) eabl7286.

[2] M. Wang, Y. Luo, T. Wang, C. Wan, L. Pan, S. Pan, K. He, A. Neo, X. Chen, Artificial skin perception, Adv. Mater. 33 (19) (2021) 2003014.

[3] W. Wang, Y. Jiang, D. Zhong, Z. Zhang, S. Choudhury, J.-C. Lai, H. Gong, S. Niu, X. Yan, Y. Zheng, et al., Neuromorphic sensorimotor loop embodied by monolithically integrated, low-voltage, soft e-skin, Science 380 (6646) (2023) 735–742.

[4] M. Cheng, G. Zhu, F. Zhang, W.-l Tang, S. Jianping, J.-q Yang, L.-y Zhu, A review of flexible force sensors for human health monitoring, J. Adv. Res. 26 (2020) 53–68.

[5] X. Liu, B. Cui, X. Wang, M. Zheng, Z. Bai, O. Yue, Y. Fei, H. Jiang, Nature-skin-derived e-skin as versatile "wound therapy-health monitoring" bioelectronic skin-scaffolds: Skin to bio-e-skin, Adv. Healthc. Mater. (2023) 2202971.

[6] T. Kim, S. Lee, T. Hong, G. Shin, T. Kim, Y.-L. Park, Heterogeneous sensing in a multifunctional soft sensor for human-robot interfaces, Sci. Robot. 5 (49) (2020) eabc6878.

[7] C. Zhao, Y. Wang, G. Tang, J. Ru, Z. Zhu, B. Li, C.F. Guo, L. Li, D. Zhu, Ionic flexible sensors: mechanisms, materials, structures, and applications, Adv. Funct. Mater. 32 (17) (2022) 2110417.

[8] H. Yao, T. Sun, J.S. Chiam, M. Tan, K.Y. Ho, Z. Liu, B.C.K. Tee, Augmented reality interfaces using virtual customization of microstructured electronic skin sensor sensitivity performances, Adv. Funct. Mater. 31 (39) (2021) 2008650.

[9] H. Kim, Y.-T. Kwon, H.-R. Lim, J.-H. Kim, Y.-S. Kim, W.-H. Yeo, Recent advances in wearable sensors and integrated functional devices for virtual and augmented reality applications, Adv. Funct. Mater. 31 (39) (2021) 2005692.

[10] Y. Chang, L. Wang, R. Li, Z. Zhang, Q. Wang, J. Yang, C.F. Guo, T. Pan, First decade of interfacial iontronic sensing: from droplet sensors to artificial skins, Adv. Mater. 33 (7) (2021) 2003464.

[11] C. Wang, C. Pan, Z. Wang, Electronic skin for closed-loop systems, ACS Nano 13 (11) (2019) 12287–12293.

[12] A.B. Dawood, H. Godaba, A. Ataka, K. Althoefer, Silicone-based capacitive e-skin for exteroception and proprioception, in: 2020 IEEE/RSJ International Conference on Intelligent Robots and Systems (IROS), IEEE, 2020, pp. 8951–8956.

[13] Z. Bai, X. Wang, M. Zheng, O. Yue, M. Huang, X. Zou, B. Cui, L. Xie, S. Dong, J. Shang, et al., Mechanically robust and transparent organohydrogel- based e-skin nanoengineered from natural skin, Adv. Funct. Mater. 33 (15) (2023) 2212856.

[14] F. Liu, S. Deswal, A. Christou, Y. Sandamirskaya, M. Kaboli, R. Dahiya, Neuro-inspired electronic skin for robots, Sci. Robot. 7 (67) (2022) eabl7344.

[15] W.-D. Li, K. Ke, J. Jia, J.-H. Pu, X. Zhao, R.-Y. Bao, Z.-Y. Liu, L. Bai, K. Zhang, M.-B. Yang, et al., Recent advances in multiresponsive flexible sensors towards e-skin: a delicate design for versatile sensing, Small 18 (7) (2022) 2103734.

[16] P. Roberts, M. Zadan, C. Majidi, Soft tactile sensing skins for robotics, Curr. Robot. Rep. 2 (2021) 343–354.

[17] Y. Chen, H. Liu, Location-dependent performance of large-area piezoresistive tactile sensors based on electrical impedance tomography, IEEE Sens. J. 21 (19) (2021) 21622–21630.

[18] Z. Yu, J. Xu, H. Gong, Y. Li, L. Li, Q. Wei, D. Tang, Bioinspired self-powered piezoresistive sensors for simultaneous monitoring of human health and outdoor uv light intensity, ACS Appl. Mater. Interfaces 14 (4) (2022) 5101–5111.

[19] Z. Ma, Y. Zhang, K. Zhang, H. Deng, Q. Fu, Recent progress in flexible capacitive sensors: structures and properties, Nano Mater. Sci. (2022).

[20] H. Shi, M. Al-Rubaiai, C.M. Holbrook, J. Miao, T. Pinto, C. Wang, X. Tan, Screen-printed soft capacitive sensors for spatial mapping of both positive and negative pressures, Adv. Funct. Mater. 29 (23) (2019) 1809116.

[21] A.J. Cheng, L. Wu, Z. Sha, W. Chang, D. Chu, C.H. Wang, S. Peng, Recent advances of capacitive sensors: materials, microstructure designs, applications, and opportunities, Adv. Mater. Technol. (2023) 2201959.

[22] K.-H. Ha, H. Huh, Z. Li, N. Lu, Soft capacitive pressure sensors: trends, challenges, and perspectives, ACS Nano 16 (3) (2022) 3442–3448.

[23] Y. Luo, L. Zhao, G. Luo, M. Li, X. Han, Y. Xia, Z. Li, Q. Lin, P. Yang, L. Dai, et al., All electrospun fabrics based piezoelectric tactile sensor, Nanotechnology 33 (41) (2022) 415502.

[24] W. Lin, B. Wang, G. Peng, Y. Shan, H. Hu, Z. Yang, Skin-inspired piezoelectric tactile sensor array with crosstalk-free row+ column electrodes for spatiotemporally distinguishing diverse stimuli, Adv. Sci. 8 (3) (2021) 2002817.

[25] N.F. Lepora, Soft biomimetic optical tactile sensing with the tactip: a review, IEEE Sens. J. 21 (19) (2021) 21131–21143.

[26] R. Wei, J. He, S. Ge, H. Liu, X. Ma, J. Tao, X. Cui, X. Mo, Z. Li, C. Wang, et al., Self-powered all optical tactile sensing platform for user-interactive interface, Adv. Mater. Technol. 8 (1) (2023) 2200757.

[27] T. He, H. Wang, J. Wang, X. Tian, F. Wen, Q. Shi, J.S. Ho, C. Lee, Self-sustainable wearable textile nano-energy nano-system (nens) for next-generation healthcare applications, Adv. Sci. 6 (24) (2019) 1901437.

[28] J.-N. Kim, J. Lee, H. Lee, I.-K. Oh, Stretchable and self-healable catechol-chitosan-diatom hydrogel for triboelectric generator and self-powered tremor sensor targeting at parkinson disease, Nano Energy 82 (2021) 105705.

[29] Q. Lu, H. Chen, Y. Zeng, J. Xue, X. Cao, N. Wang, Z. Wang, Intelligent facemask based on triboelectric nanogenerator for respiratory monitoring, Nano Energy 91 (2022) 106612.

[30] Y. Yan, Z. Hu, Z. Yang, W. Yuan, C. Song, J. Pan, Y. Shen, Soft magnetic skin for super-resolution tactile sensing with force self-decoupling, Sci. Robot. 6 (51) (2021) eabc8801.

[31] J. Man, G. Chen, J. Chen, Recent progress of biomimetic tactile sensing technology based on magnetic sensors, Biosensors 12 (11) (2022) 1054.

[32] O. Atalay, A. Atalay, J. Gafford, C. Walsh, A highly sensitive capacitive-based soft pressure sensor based on a conductive fabric and a microporous dielectric layer, Adv. Mater. Technol. 3 (1) (2018) 1700237.

[33] S. Zhao, W. Ran, D. Wang, R. Yin, Y. Yan, K. Jiang, Z. Lou, G. Shen, 3d dielectric layer enabled highly sensitive capacitive pressure sensors for wearable electronics, ACS Appl. Mater. Interfaces 12 (28) (2020) 32023–32030.

[34] H. Niu, S. Gao, W. Yue, Y. Li, W. Zhou, H. Liu, Highly morphology-controllable and highly sensitive capacitive tactile sensor based on epidermis-dermis inspired interlocked asymmetric-nanocone arrays for detection of tiny pressure, Small 16 (4) (2020) 1904774.

[35] T. Someya, M. Amagai, Toward a new generation of smart skins, Nat. Biotechnol. 37 (4) (2019) 382–388.

[36] Q. Su, Q. Zou, Y. Li, Y. Chen, S.-Y. Teng, J.T. Kelleher, R. Nith, P. Cheng, N. Li, W. Liu, et al., A stretchable and strain-unperturbed pressure sensor for motion interference–free tactile monitoring on skins, Sci. Adv. 7 (48) (2021) eabi4563.

[37] B. Nie, S. Liu, Q. Qu, Y. Zhang, M. Zhao, J. Liu, Bio-inspired flexible electronics for smart e-skin, Acta Biomater. 139 (2022) 280–295.

[38] S.R.A. Ruth, L. Beker, H. Tran, V.R. Feig, N. Matsuhisa, Z. Bao, Rational design of capacitive pressure sensors based on pyramidal microstructures for specialized monitoring of biosignals, Adv. Funct. Mater. 30 (29) (2020) 1903100.

[39] Y. Luo, J. Shao, S. Chen, X. Chen, H. Tian, X. Li, L. Wang, D. Wang, B. Lu, Flexible capacitive pressure sensor enhanced by tilted micropillar arrays, ACS Appl. Mater. Interfaces 11 (19) (2019) 17796–17803.

[40] P. Nie, R. Wang, X. Xu, Y. Cheng, X. Wang, L. Shi, J. Sun, High-performance piezoresistive electronic skin with bionic hierarchical microstructure and microcracks, ACS Appl. Mater. Interfaces 9 (17) (2017) 14911–14919.

[41] J. Shi, L. Wang, Z. Dai, L. Zhao, M. Du, H. Li, Y. Fang, Multiscale hierarchical design of a flexible piezoresistive pressure sensor with high sensitivity and wide linearity range, Small 14 (27) (2018) 1800819.

[42] Y. Wan, Z. Qiu, Y. Hong, Y. Wang, J. Zhang, Q. Liu, Z. Wu, C.F. Guo, A highly sensitive flexible capacitive tactile sensor with sparse and high- aspect-ratio microstructures, Adv. Electron. Mater. 4 (4) (2018) 1700586.

[43] Y. Zhang, J. Yang, X. Hou, G. Li, L. Wang, N. Bai, M. Cai, L. Zhao, Y. Wang, J. Zhang, et al., Highly stable flexible pressure sensors with a quasi-homogeneous composition and interlinked interfaces, Nat. Commun. 13 (1) (2022) 1317.

[44] U. Pierre Claver, G. Zhao, Recent progress in flexible pressure sensors based electronic skin, Adv. Eng. Mater. 23 (5) (2021) 2001187.

[45] C. Liu, J.J. Busfield, K. Zhang, An electric self- sensing and variable-stiffness artificial muscle, Adv. Intell. Syst. (2023) 2300131.

[46] Y. Li, M. Guo, Y. Li, Recent advances in plasticized pvc gels for soft actuators and devices: a review, J. Mater. Chem. C 7 (42) (2019) 12991–13009.

[47] T. Hwang, Z. Frank, J. Neubauer, K.J. Kim, High- performance polyvinyl chloride gel artificial muscle actuator with graphene oxide and plasticizer, Sci. Rep. 9 (1) (2019) 9658.

[48] T. Dong, T. Liu, The electrical response and self- sensing of the fully flexible pvc gel actuator based on flexible electrodes, Sens. Actuators A: Phys. 340 (2022) 113554.

[49] M.A. Sharif, Pvc gel smart sensor for robotics sensing applications: an experimental and finite element simulation study, Eng. Res. Express 4 (3) (2022) 035029.

[50] Y.J. Son, J.W. Bae, H.J. Lee, S. Bae, S. Baik, K.-Y. Chun, C.-S. Han, Humidity-resistive, elastic, transparent ion gel and its use in a wearable, strain- sensing device, J. Mater. Chem. A 8 (12) (2020) 6013–6021.

[51] H. Park, S.-J. Oh, D. Kim, M. Kim, C. Lee, H. Joo, Woo, J.W. Bae, J.-H. Lee, Plasticized pvc-gel single layer-based stretchable triboelectric nanogenerator for harvesting mechanical energy and tactile sensing, Adv. Sci. 9 (22) (2022) 2201070.

[52] R. Yang, W. Zhang, N. Tiwari, H. Yan, T. Li, H. Cheng, Multimodal sensors with decoupled sensing mechanisms, Adv. Sci. 9 (26) (2022) 2202470.

[53] S. Lee, S. Franklin, F.A. Hassani, T. Yokota, M.O.G. Nayeem, Y. Wang, R. Leib, G. Cheng, D.W. Franklin, T. Someya, Nanomesh pressure sensor for monitoring finger manipulation without sensory interference, Science 370 (6519) (2020) 966–970.

[54] M. Ali, T. Ueki, D. Tsurumi, T. Hirai, Influence of plasticizer content on the transition of electrome-chanical behavior of pvc gel actuator, Langmuir 27 (12) (2011) 7902–7908.

[55] H. Ouyang, Z. Li, M. Gu, Y. Hu, L. Xu, D. Jiang, S. Cheng, Y. Zou, Y. Deng, B. Shi, et al., A bioresorbable dynamic pressure sensor for cardiovascular postoperative care, Adv. Mater. 33 (39) (2021) 2102302.

[56] J. Van Kuilenburg, M.A. Masen, E. Van Der Heide, Contact modelling of human skin: What value to use for the modulus of elasticity? Proc. Inst. Mech. Eng. Part J: J. Eng. Tribol. 227 (4) (2013) 349–361.

[57] A. Kalra, A. Lowe, A.A. Jumaily, An overview of factors affecting the skins youngs modulus, J. Aging Sci. 4 (2) (2016) 1000156.

[58] X. Yang, S. Chen, Y. Shi, Z. Fu, B. Zhou, A flexible highly sensitive capacitive pressure sensor, Sens. Actuators A: Phys. 324 (2021) 112629.

[59] Z. Feng, Q. He, X. Wang, Y. Lin, J. Qiu, Y. Wu, J. Yang, Capacitive sensors with hybrid dielectric structures and high sensitivity over a wide pressure range for monitoring biosignals, ACS Appl. Mater. Interfaces 15 (4) (2023) 6217–6227.
[60] P. Yu, X. Li, H. Li, Y. Fan, J. Cao, H. Wang, Z. Guo, X. Zhao, Z. Wang, G. Zhu, All-fabric ultrathin capacitive sensor with high pressure sensitivity and broad detection range for electronic skin, ACS Appl. Mater. Interfaces 13 (20) (2021) 24062–24069.
[61] R. Qin, M. Hu, X. Li, T. Liang, H. Tan, J. Liu, G. Shan, A new strategy for the fabrication of a flexible and highly sensitive capacitive pressure sensor, Microsyst. Nanoeng. 7 (1) (2021) 100.

Chen Liu received the B.E. degree in process equipment and control engineering from Northwest University, Xi'an, China, in 2017, and the M.E. degree in mechanical engineering from Xi'an Jiaotong University, Xi'an, China, in 2020. He is currently pursuing a Ph.D. degree in mechanical engineering at Queen Mary University of London, London, UK. His research interests include soft robotics, smart actuators, and flexible sensors.

Muhammad Hassan Uddin received the B.S. degree in mechanical engineering from Queen Mary University of London, UK, in 2023.

Ketao Zhang is a Senior Lecturer at Queen Mary, University of London (QMUL), and is the Director of the Robotic Systems Research Group, a core robotics team within the Centre for Advanced Robotics @ QMUL (ARQ). His research explores design theory of mechanisms, reconfigurable parallel manipulators, morphable soft-bodied robots, autonomous mobile manipulators, and aerial robots that can operate in dynamic and challenging environments.